Journal of Sound and Vibration (2002) **254**(2), 393–406
doi:10.1006/jsvi.2001.4101, available online at http://www.idealibrary.com on IDEAL®

ON THE DESIGN OF BARS AND BEAMS FOR DESIRED MODE SHAPES

E. Lai and G. K. Ananthasuresh

Department of Mechanical Engineering and Applied Mechanics, The University of Pennsylvania, 297 Towne Building, 220 S. 33rd Street, Philadelphia, PA 19104-6315, *U.S.A.*

(*Received* 10 *May* 2000, *and in final form* 29 *August* 2001)

1. INTRODUCTION

The natural frequencies and normal mode shapes become important in devices that are subject to vibration and in those that operate at high speeds in the dynamic regime. Some devices, especially at micro scale in micro-electro-mechanical systems (MEMS), are intentionally operated at resonance frequencies to enhance their performance. Optimizing the structural elements in order to have desired frequencies is of interest in some applications at both the macro and micro scales. This "inverse frequency" problem is studied extensively [1], including the topology optimization problem [2]. The "inverse mode shape" problem, on the other hand, entails the determination of the geometry of the structure such that it will have prescribed mode shapes. There are applications where a particular mode shape is critical for the performance of the device. This is especially true in the design of resonance-based micro accelerometers and gyroscopes where sensing is accomplished through capacitance measurement, which is very sensitive to the geometry of elastically deforming structures. For instance, in the micro rate gyroscope [3], the mode shape of a ring structure can be optimized to improve the performance. Designing the shape of the cantilever probes on the atomic force microscope to attain a desired modal deflection is another example [4]. In micro locomotion systems (e.g., swimming) where repeated changes in shape propel the whole entity forward [5], energy efficiency can be achieved by designing the structure such that the normal mode shapes are the same as the required repetitive shape changes. At macro scale, the inverse mode shape problem can be used to design the tooling for manufacturing equipment such that vibratory displacement is minimized in certain directions. Currently, there do not appear to be any general systematic methods to design the geometry of the structures for desired mode shapes.

Compared to the inverse frequency problem, the inverse mode shape problem has received much less attention. The inverse mode shape problem arises in two different settings. In the first category, the experimentally obtained eigendata (natural frequencies and mode shapes) of the structures is used for the characterization of their geometry and material density. Efforts in this direction are found in references [6–14]. In the second category, which is the focus of this paper, the geometry of the structure is designed for prescribed mode shapes using a given material. Efforts in this direction are found in references [4, 15]. It should be noted that an arbitrarily specified mode shape might not always be physically realizable with a given class of structures such as strings, cables, rods, and frames consisting of straight and curved beams, plates and membranes, shells and general 3-D structures. Consequently, in the second category of "the design for desired mode shape problems", the prescribed mode shape should be checked against a set of criteria that ensure physical realizability.

0022-460X/02/$35.00

In the following sections, after a brief description of the related work, the inverse mode shape problem of bars and beams will be discussed. The area profile of an axially vibrating bar is solved by two methods: analytical solution of the continuous model, and a numerical method using a discretized finite element model. This is followed by the inverse mode shape problem for the cantilever beam. A list of criteria for the mode shape to ensure physical realizability of the cross-sectional area is then presented along with the formulation of the optimization program for mode shape modification to render it physically realizable. The method is demonstrated with an example of designing the cross-sectional area of a cantilever beam for a prescribed mode shape.

2. RELATED WORK

As mentioned previously, the inverse vibration problem includes both the inverse frequency (eigenvalue) and inverse mode shape (eigenvector) problem. The inverse eigenvalue problem has been addressed by several researchers [16–19]. Barcilon incorporated eigenvector data into the reconstruction process of a discrete spring–mass model of a bar from three eigenvectors and their corresponding eigenvalues associated with three boundary conditions [20–22]. Ross introduced a procedure for deriving both the mass and stiffness matrices from experimentally measured natural frequencies and a square modal matrix composed of measured mode vectors supplemented by arbitrary linearly independent vectors [6]. Gladwell derived the necessary and sufficient conditions applicable to the spectral data (eigenvalues and the corresponding eigenvectors) to permit the construction of a realizable beam [23]. Gladwell and Gbadeyan have shown that a simply connected spring–mass system, fixed at one end and free at the other, may be reconstructed uniquely from two eigenvalues, two eigenvectors and the total mass of the system [24]. Two sets of eigenvalues and eigenvectors for the fixed–fixed and fixed–free boundary conditions can be used to reconstruct the mass and stiffness matrices of a discrete finite difference model of the non-uniform axially vibrating bar uniquely. Ram and Caldwell showed that the physical parameters of a free multi-connected spring–mass system could be determined from certain spectral sequences as well [10]. The inverse mode problem for the continuous model of an axially vibrating bar from two eigenvalues, the corresponding eigenvectors and the total mass of the system was solved by Ram [12]. Ram and Gladwell proposed a way to reconstruct a finite element model of a vibrating bar from a single eigenvalue and two eigenvectors based on the fact that both the mass and stiffness matrices of the finite element model are tri-diagonal [14]. Ram also showed a method of reconstructing a finite difference model of a vibrating beam from three eigenvectors, one eigenvalue and the total mass of the beam [13].

The motivation of the Ram and Gladwell work, and other references was to recover the density and shape information from experimental eigendata of the structure. As mentioned above, the focus of this paper is on the design problem of inverse mode shape problem where the material density is uniform throughout and the specified mode shapes should be checked for physical realizability. This paper is limited to axially deforming bars and transversely deforming beams.

3. INVERSE MODE SHAPE PROBLEM FOR BARS

3.1. INVERSE PROBLEM FOR THE CONTINUOUS MODEL OF A BAR

Consider the governing equation for the free axial vibration $v(x)$ of a bar:

$$\frac{\mathrm{d}}{\mathrm{d}x}\left[EA(x)\frac{\mathrm{d}v}{\mathrm{d}x}\right] + \rho A(x)\lambda v(x) = 0, \tag{1}$$

TABLE 1

Areas of cross-sections for prescribed mode shapes of an axially deforming bar

Example 1	$v = \sin\left(\frac{\pi x}{2L}\right), \quad \psi(x) = \dfrac{E\left(-\frac{\pi^2}{4L^2}\sin\left(\frac{\pi x}{2L}\right)\right) + \rho = \left(\frac{E\pi^2}{4\rho L^2}\right)\sin\left(\frac{\pi x}{2L}\right)}{E\frac{\pi}{2L}\cos\left(\frac{\pi x}{2L}\right)}$
	$\lambda = \dfrac{E\pi^2}{4\rho L^2}, \quad A(x) = \mathrm{e}^{-\int 0\,\mathrm{d}x} = C\mathrm{e}^0 = C$
Example 2	$v = -(x-1)^2 + 1, \quad \psi(x) = \dfrac{2 - (\rho\lambda/E)x(2-x)}{2(x-1)}$
	$\lambda = 2\dfrac{E}{\rho}, \quad A = C\mathrm{e}^{x - 1/2x^2}$
Example 3	$v = x - x^2, \quad \psi(x) = \dfrac{-2 + \rho\lambda/E(x - x^2)}{(1-2x)}$
	$\lambda = 8\dfrac{E}{\rho}, \quad A = C\mathrm{e}^{2(x-x^2)}$
Example 4	$v = \dfrac{1}{3}x^3 - \dfrac{1}{2}(1+s)x^2 + sx; \quad \psi(x)$
	$= \dfrac{E(2x - (s+1)) + \lambda\rho x/6(2x^2 - 3(s+1)x + 6s)}{E(x-1)(x-s)} = (p + qx)$
	$\lambda = \dfrac{6E(2+\sqrt{3})}{\rho}; \quad s = 1/(2+\sqrt{3}); \quad p = -3 - \sqrt{3}; \quad q = 4 + 2\sqrt{3}$
	$A(x) = \mathrm{e}^{((3+\sqrt{3})x - (2+\sqrt{3})x^2)}$

where $A(x) > 0$ and $\rho > 0$ are the cross-sectional area and density of the bar, respectively, and λ is the square of the natural frequency. Ram derived the cross-sectional area $A(x)$ and density $\rho(x)$ of an axially vibrating bar using two interrelated eigenvectors obtained from different boundary conditions, their corresponding eigenvalues and the total mass of the system [12]. In contrast to Ram's work, in the design problem considered here, the density along the bar is assumed to be constant and only one eigenvector is specified. We assume that $A(x)$ is a differentiable function in the closed interval $0 \leqslant x \leqslant L$, where L is the total length of the bar. Equation (1) can be re-written in terms of the cross-sectional area as

$$A'(x) + \frac{[Ev''(x) + \rho\lambda v(x)]}{Ev'(x)} A(x) = 0, \tag{2}$$

where the primes denote the derivative with respect to x. By defining a function, ψ, as

$$\psi(x) = \frac{Ev''(x) + \rho\lambda v(x)}{Ev'(x)}. \tag{3}$$

We can solve for the area of cross-section in equation (2) as shown below:

$$A(x) = C\mathrm{e}^{-\int \psi(x)\,\mathrm{d}x}, \tag{4}$$

where C is a constant of integration that can be determined uniquely from the total mass of the bar as

$$Mass = m = \rho \int_0^L A(x)x \ \mathrm{d}x. \tag{5}$$

The condition to ensure that $A(x)$ is positive is that $\psi(x)$ must be finite for all x in the interval $0 \leqslant x \leqslant L$. Further restriction on the desired mode shape is that it should satisfy the boundary conditions of the bar. Table 1 shows four examples with fixed–fixed and fixed–free boundary conditions. These examples show that the aforementioned condition on $\psi(x)$ determines the value of λ when a mode shape is prescribed. The condition on $\psi(x)$ manifests because of the presence of $v'(x)$ in the denominator as can be seen in equation (3). So, when a prescribed mode shape has a zero first derivative anywhere in the interval $0 \leqslant x \leqslant L$, λ should be chosen such that either the numerator of $\psi(x)$ is zero for the entire interval as in example 1, or that $v'(x)$ should be cancelled out as a factor from the numerator as in the other three examples (see Table 1). This restriction of the natural frequency can also be seen in the discretized model, which will be presented next.

3.2. DISCRETIZED MODEL FOR A FIXED–FIXED BAR

The discretized form of equation (1) is given by

$$(\mathbf{K} - \lambda \mathbf{M})\mathbf{u} = 0, \tag{6}$$

where $\mathbf{K}$ and $\mathbf{M}$ are stiffness and inertia matrices, respectively, $\mathbf{u}$ is the mode shape vector, and λ is the square of the natural frequency. The mass and stiffness matrices can be written in terms of the bar's cross-sectional area and given material properties. When the bar is divided into N finite elements, there will be N unknowns $A_i (i = 1, 2, \ldots, N)$ denoting the cross-section areas of elements. There will be $(N + 1)$ nodes numbered $0, 1, \ldots, N$ with zeroth and Nth nodes specified to be zero for the fixed–fixed boundary condition. Therefore, the mode shape vector $\mathbf{u}$ in equation (6) is of the size $(N - 1) \times 1$ after the boundary conditions are applied. The stiffness and inertia matrices for the fixed–fixed condition are given by

$$\mathbf{K} = \begin{bmatrix} k_1 + k_2 & -k_2 & & & & \\ -k_2 & k_2 + k_3 & -k_3 & & & \\ & -k_3 & k_3 + k_4 & \ddots & & \\ & & \ddots & \ddots & -k_{N-1} & \\ & & & -k_{N-1} & k_{N-1} + k_N & \end{bmatrix}_{(N-1)\times(N-1)}, \tag{7a}$$

$$\mathbf{M} = \begin{bmatrix} 2m_1 + 2m_2 & m_2 & & & & \\ m_2 & 2m_2 + 2m_3 & m_3 & & & \\ & m_3 & 2m_3 + 2m_4 & \ddots & & \\ & & \ddots & \ddots & m_{N-1} & \\ & & & m_{N-1} & 2m_{N-1} + 2m_N & \end{bmatrix}_{(N-1)\times(N-1)}, \tag{7b}$$

where $m_i = \rho A_i l/6$ and $k_i = E A_i/l$ in which E is Young's Modulus, l is the length of each element, and ρ is the density. Since the A_i's are unknowns now, equation (6) can be

re-written so that the displacements u_i appear in a matrix and the A_i's in the unknown vector as

$$\mathbf{PA} = \begin{bmatrix} P_{1,1} & P_{1,2} & 0 & 0 & 0 & \cdots & 0 \\ 0 & P_{2,2} & P_{2,3} & 0 & 0 & \cdots & 0 \\ 0 & 0 & P_{3,3} & P_{3,4} & 0 & \cdots & 0 \\ \vdots & \vdots & \vdots & \ddots & \vdots & \vdots & \vdots \\ 0 & 0 & 0 & \cdots & P_{N-2,N-2} & P_{N-2,N-1} & 0 \\ 0 & 0 & 0 & \cdots & 0 & P_{N-1,N-1} & P_{N-1,N} \end{bmatrix}_{(N-1)\times N} \begin{bmatrix} A_1 \\ A_2 \\ A_3 \\ \vdots \\ A_N \end{bmatrix}_{N\times 1} = \mathbf{0}, \tag{8}$$

where $P_{1,1} = cu_1$, $P_{1,2} = cu_1 - du_2$, $P_{i,i} = cu_i - du_{i-1}$, $P_{i,i+1} = cu_i - du_{i+1}$, *for* $i = 2, 3, \ldots, N-2$, $P_{N-1,N-1} = cu_{N-1} - du_{N-2}$, $P_{N-1,N} = cu_{N-1}$, *with* $c = E/l - \lambda\rho l/3$, $d = E/l + \rho\lambda l/6$.

Since **P** has the deficiency of rank by 1, its nullspace can be constructed to obtain the non-trivial solution for **A**. Without loss of generality, if we assume that A_N is unity, each row of equation (8) can be solved to obtain the next elemental area of cross-section as

$$\frac{A_2}{A_1} = \frac{cu_1}{du_2 - cu_1}, \quad \frac{A_{i+1}}{A_i} = \frac{cu_i - du_{i-1}}{du_{i+1} - cu_i}, \frac{A_N}{A_{N-1}} = \frac{cu_{N-1}}{du_{N-2} - cu_{N-1}} \quad \textit{for } i = 2, 3, \ldots, N-2. \tag{9}$$

The relationships between successive A_i's in equation (9) also serve as the conditions for the physical realizability of a given mode shape. If all these ratios are positive and finite, then the mode shape is physically realizable. This is equivalent to the condition on $\psi(x)$ described earlier with the continuous model of the bar. Since the constants c and d (see equation (8)) depend on the natural frequency, the physical reliability condition restricts the value λ for a given material. The solution to the area profile is not yet unique because all of the A_i's can be multiplied by a scale factor without changing the frequency or the mode shape. In order to determine this scale factor, the total weight for the structure W_{total} could be used, which is given by the relationship

$$W_{total} = \rho l \sum_{i=1}^{N} A_i \,. \tag{10}$$

3.3. DISCRETIZED MODEL FOR A FIXED–FREE BAR

The discretized formulation of the fixed–free case is similar to that of the fixed–fixed case with a small difference. First, the stiffness and inertia matrices are given by

$$\mathbf{K} = \begin{bmatrix} k_1 + k_2 & -k_2 & & & & \\ -k_2 & k_2 + k_3 & -k_3 & & & \\ & \ddots & \ddots & \ddots & & \\ & & -k_{N-1} & k_{N-1} + k_N & -k_N & \\ & & & -k_N & k_N \end{bmatrix}_{N\times N}, \tag{11a}$$

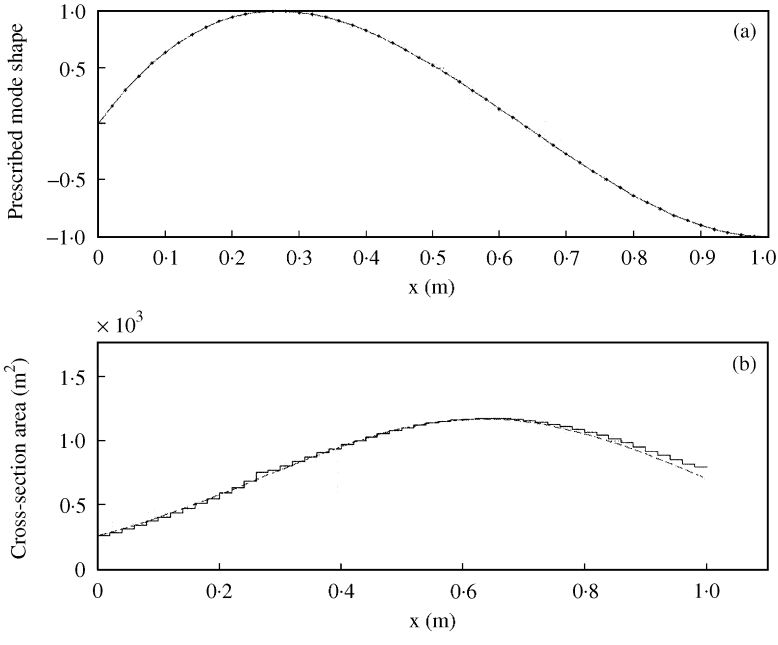

Figure 1. (a) Prescribed second mode shape vector and (b) the cross-section area using the discretized model for the fixed–free bar (——, discretized; – – –, exact).

$$\mathbf{M} = \begin{bmatrix} 2m_1 + 2m_2 & m_2 & & & & \\ m_2 & 2m_2 + 2m_3 & m_3 & & & \\ & \ddots & \ddots & \ddots & & \\ & & m_{N-1} & 2m_{N-1} + 2m_N & m_N & \\ & & & m_N & 2m_N & \end{bmatrix}_{N \times N} \tag{11b}$$

for N elements with cross-section areas $A_i (i = 1, 2, \ldots, N)$ and $(N + 1)$ nodes numbered $0, 1, \ldots, N$ with zeroth node specified to be zero. The size of the mode shape vector $\mathbf{u}$ is now $N \times 1$. Therefore, in the rearranged form that is similar to equation (8), there are N unknown A_i and N equations. That is,

$$\mathbf{P}_{N \times N} \mathbf{A}_{N \times 1} = 0. \tag{12}$$

The last row of the above equation can be used to solve for λ:

$$\lambda = \frac{6E(-u_{N-1} + u_N)}{\rho L^2 (u_{N-1} + 2u_N)}. \tag{13}$$

This means that the natural frequency is automatically determined when a mode shape is prescribed for a fixed–free bar. In the continuous model, by applying the free-end boundary condition ($v'_{x=L} = 0$) to equation (2), we can see that $\lambda = (-E/\rho)(v''/v)_{x=L}$. Using the remaining $(N - 1)$ rows of equation (12), the following recurrence relationship can be obtained:

$$A_i = \frac{((\lambda \rho l^2/6E)(2u_i + u_{i+1}) - (u_i - u_{i+1}))}{((u_i - u_{i-1}) - (\lambda \rho l^2/6E)(2u_{i-1} + u_i))} A_{i+1} \quad \text{for} \quad i = 1, \ldots, N - 1. \tag{14}$$

As before, without loss of generality, A_N can be assumed to be unity to successively determine the remaining A_i using equation (14), and then by knowing the total mass W_{total} of the bar, we can compute the scale factor for the areas. Equation (14) also serves as the condition for physical realizability of a mode shape because the ratios of areas of cross-section of successive elements should be positive and finite.

Examples in Table 1 were also solved using the discretized finite element models and were compared with the exact solutions of the continuous model. The solution for example 4 along with the prescribed mode shape is shown in Figure 1. The following data was used in this example: length of the bar = 1 m; Young's modulus = $E = 210$ GPa; density = $\rho = 2300\ \text{kg/m}^3$; weight of the bar = $W = 2$ kg, and $N = 50$. In this and other examples, the numerical solutions from the discretized model approach the exact solution with an increasing number of elements and thus are validated.

4. INVERSE MODE SHAPE PROBLEM FOR BEAMS

As in the case of bars, in beams too arbitrarily specified mode shapes do not result in physically meaningful geometries. The conditions for a valid mode shape depend on the boundary conditions of the beam. The discussion in this paper is limited to the case of a cantilever beam for which the governing differential equation for free vibration is given by

$$\frac{\mathrm{d}^2}{\mathrm{d}x^2}\left(EI\frac{\mathrm{d}^2u}{\mathrm{d}x^2}\right) - \lambda\rho Au = 0, \quad \lambda = \omega^2, \tag{15}$$

where $I(x)$ and $A(x)$ are the second moment of inertia and area of cross-section along the longitudinal axis of the beam respectively; E, L and ρ are Young's modulus, length, and density of the beam; $u(x)$ is the mode shape corresponding to a frequency ω. Discretization of this equation using the finite difference method gives rise to the matrix eigenvalue problem

$$\mathbf{Ku} = \lambda\mathbf{Mu}, \tag{16}$$

where the inertia matrix $\mathbf{M}$ is a diagonal matrix with diagonal entries $m_1 = \rho A_i l$, and the stiffness matrix $\mathbf{K} = \mathbf{E}\mathbf{L}^{-1}\mathbf{E}\bar{\mathbf{K}}\mathbf{E}^{\mathrm{T}}\mathbf{L}^{-1}\mathbf{E}^{\mathrm{T}}$ is the pentadiagonal as shown below [13]:

$$\mathbf{K} = \begin{bmatrix} a_1 & -b_1 & c_1 & 0 & 0 & \cdots & 0 & 0 \\ -b_1 & a_2 & -b_2 & c_2 & 0 & \cdots & 0 & 0 \\ c_1 & -b_2 & a_3 & -b_3 & c_3 & \cdots & 0 & 0 \\ 0 & c_2 & -b_3 & a_4 & -b_4 & \cdots & 0 & 0 \\ \vdots & \vdots & \vdots & \vdots & \vdots & \ddots & \vdots & \vdots \\ 0 & 0 & 0 & 0 & 0 & \cdots & a_{N-1} & -b_{N-1} \\ 0 & 0 & 0 & 0 & 0 & \cdots & -b_{N-1} & a_N \end{bmatrix} \tag{17}$$

with coefficients

$$a_i = (k_i + 4k_{i+1} + k_{i+2})/l^2,\ b_i = (k_{i+1} + k_{i+2})/l^2,\ c_i = k_{i+2}/l^2$$

and $\bar{\mathbf{K}} = \text{diag}(k_i)$ with $k_i = Eh^2 A_i/l^3$; L = identity matrix multiplied by l, and

$$\mathbf{E} = \begin{bmatrix} 1 & -1 & 0 & \cdots & 0 \\ 0 & 1 & -1 & \cdots & 0 \\ \cdot & \cdot & \cdot & \cdot & \cdot \\ 0 & \cdots & \cdots & 1 & -1 \\ 0 & \cdots & \cdots & 0 & 1 \end{bmatrix}.$$

The above discretization assumed finite difference grid spacing of length l where A_i is the area of cross-section across the ith grid spacing. A rectangulr cross-section was assumed with thickness h while the width is assumed to vary along the axis. The transverse displacement in the mode shape is given by $\mathbf{u} = \{u_1, u_2, \ldots, u_N\}$. The inertia and stiffness matrices together with the mode shape vector $\mathbf{u}$ can be re-written so that the modal displacements u_i appear in the matrices and A_i as the unknown vector:

$$\mathbf{CA} = \begin{bmatrix} C_{11} & C_{12} & C_{13} & 0 & 0 & \cdots & 0 \\ 0 & C_{22} & C_{23} & C_{24} & 0 & \cdots & 0 \\ \vdots & \vdots & \ddots & \vdots & \vdots & \cdots & 0 \\ 0 & 0 & \cdots & 0 & C_{N-2,N-2} & C_{N-2,N-1} & C_{N-2,N} \\ 0 & 0 & \cdots & 0 & 0 & C_{N-1,N-1} & C_{N-1,N} \\ 0 & 0 & \cdots & 0 & 0 & 0 & C_{N,N} \end{bmatrix}_{N\times N} \begin{bmatrix} A_1 \\ A_2 \\ A_3 \\ \vdots \\ A_N \end{bmatrix}_{N\times 1} = \mathbf{0},$$

where

$$C_{1,1} = \frac{Eh^2}{12l^3} u_1 - \rho\lambda l u_1,\ C_{i,i+1} = \frac{Eh^2}{6l^3}(u_{i-1} - 2u_i + u_{i+1}),\ C_{i,i+2} = \frac{Eh^2}{12l^3}(u_i - 2u_{i+1} + u_{i+2}),$$

$$C_{i,i} = \frac{Eh^2}{12l^3}(u_{i-2} - 2u_{i-1} - u_i) - \rho\lambda l u_i,\ C_{N,N} = \frac{Eh^2}{12l^3}(u_{N-2} - 2u_{N-1} - u_N) - \rho\lambda l u_N. \quad (18)$$

The eigenvalue λ can be determined by solving the last row of the above equation:

$$\lambda = \frac{Eh^2}{12\rho l^4} \frac{(u_{N-2} - 2u_{N-1} + u_N)}{u_N}. \quad (19)$$

Thus, as in the case of the bars, the frequency cannot be arbitrarily chosen when a mode shape is specified. The remaining rows of equations can be solved sequentially starting from the second row from bottom and moving up to get

$$A_{N-1} = -\frac{C_{N-1,N}}{C_{N-1,N-1}},\quad A_i = -\frac{(C_{i,i+1}A_{i+1} + C_{i,i+2}A_{i+2})}{C_{i,i}}. \quad (20)$$

Equation (20) also serves as conditions on a given mode shape vector for obtaining positive areas. The solution to the area profile is not yet unique because all areas can be multiplied by a scaled factor without changing the eigenvector. In order to determine this scale factor, the total weight of the beam W_{total} should be known as in the case of bars.

5. CRITERIA FOR THE PHYSICAL REALIZABILITY OF BEAM MODE SHAPES

Since eigenvalue computed using equation (19) should be positive, one condition for a valid mode shape is readily obtained. This and other conditions can be more easily seen from the

differential equation of equation (15) which can be re-written in terms of $A(x)$ as

$$u''A''(x) + 2u'''A'(x) + \left(u^{IV} - \frac{12\rho\lambda}{Eh^2}u\right)A(x) = 0, \quad 0 \leqslant x \leqslant L. \tag{21}$$

At the free end of the cantilever beam, i.e., when $x = L$, the boundary conditions dictate that $u''_L = u'''_L = 0$ to have zero bending moment and shear force. This simplifies equation (21) to

$$\left(u_L^{IV} - \frac{12\rho\lambda}{Eh^2}u_L\right)A(L) = 0. \tag{22}$$

The square of the natural frequency λ can be found if the area profile at $A(L) \neq 0$,

$$\lambda = \frac{Eh^2}{12\rho}\frac{u_L^{IV}}{u_L}, \tag{23}$$

which would agree with λ obtained from the finite difference formulation in equation (17) if the fourth derivative is approximated as $u_N^{IV} = (u_{N-2} - 2u_{N-1} + u_N)/l^4$ in the finite difference model. This and other conditions to be satisfied by the prescribed mode shape $u(x)$ are listed below:

(1) The mode shape and its first four derivatives must be smooth and continuous.
(2) $u(x)$ must satisfy the boundary conditions: $u_0 = u'_{0L} = 0$ at $x = 0$ and $u''_L = u'''_L = 0$ at $x = L$.
(3) The number of sign changes in the mode shape and the first derivative along the length of the beam must be the same [8].
(4) $(uu^{IV}) > 0$ at the free end of the beam to ensure positive eigenvalue.

An example illustrates the application of these conditions to a mode shape design problem.

6. BEAM EXAMPLE

For design purposes, the user does not specify a continuous mode shape but, instead, specifies a set of prescribed points. In order to use the method described in section 4 for obtaining the area profile, the prescribed points are fitted onto a smooth curve that satisfies the boundary conditions for the beam. The choice of parameterization should be chosen such that the four derivatives are continuous and fit well to the prescribed points. In this example, the mode shape is considered as a sixth order polynomial with unknown coefficients a_i:

$$u(x) = a_0 + a_1x + a_2x^2 + a_3x^3 + a_4x^4 + a_5x^5 + a_6x^6. \tag{24}$$

By applying boundary conditions $u_0 = u'_0 = u''_L = u'''_L = 0$ and solving for the unknown coefficients, the polynomial depends only on three coefficients: a_4, a_5 and a_6:

$$\begin{aligned} u(x) = {} & (6a_4L^2 + 20a_5L^3 + 45a_6L^4)x^2 \\ & - 2(2a_4L + 5a_5L^2 + 10a_6L^3)x^3 \\ & + a_4x^4 + a_5x^5 + a^6x^6. \end{aligned} \tag{25}$$

To ensure that λ is positive, criterion (4) must be satisfied so that

$$u_Lu_L^{IV} = 24L^2(3a_4 + 11a_5 + 26a_6L^2)(a_4 + 5a_5 + 15a_6L^2) > 0. \tag{26}$$

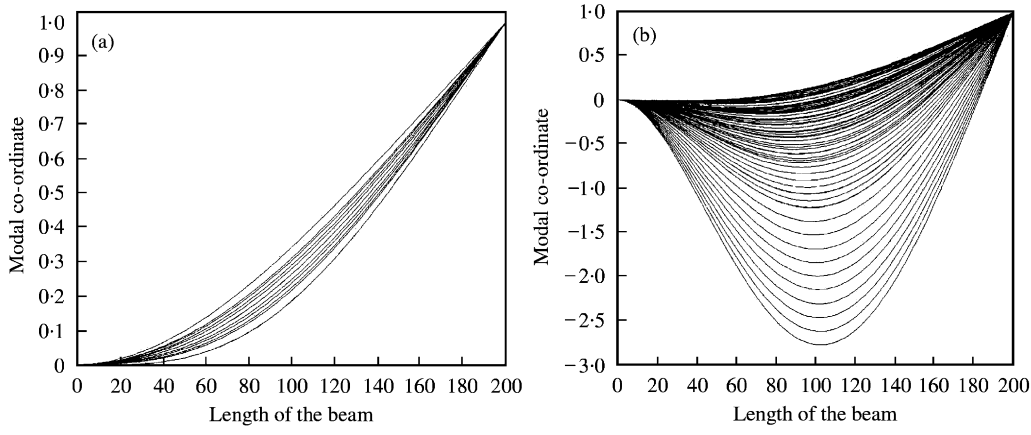

Figure 2. (a) A family of plausible primary mode shapes for a range of a_4, a_5 and a_6 for a given beam length of $L = 200$. (b) A family of plausible secondary mode shapes.

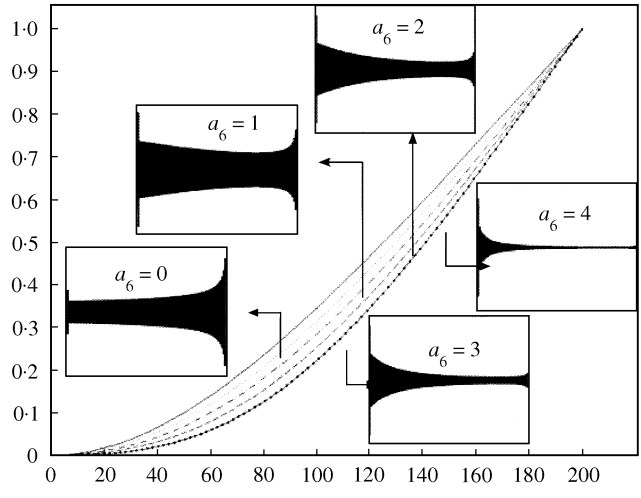

Figure 3. A family of first mode shapes for a range of a_4, a_5 and a_6 for a cantilever beam length of $L = 200$ along with their area profiles (——, $a_6 = 0$; . . . ., 1; —·—, 2; – – –, 3; ——, 4).

To explore the feasible choices of a_4, a_5 and a_6 for satisfying the above inequality, we let $v_1 = (3a_4 + 11a_5L)/26L^2$ and $v_2 = (a_4 + 5a_5L)/15L^2$ such that the inequality takes the form

$$u_L u_L^{IV} = 24(26)(15)L^2(a_6 + v_1)(a_6 + v_2) > 0. \tag{27}$$

Using the above condition on a_6 and by varying the values of a_4 and a_5 a family of valid mode cantilever mode shapes are obtained and plotted in Figure 2. The figure shows both the fundamental (Figure 2(a)) and the second (Figure 2(b)) mode shapes. To further examine how the choice of a_4, a_5 and a_6 affects the mode shape and the reconstructed area profile, a few fundamental mode shapes from the family of mode shapes are selected and are shown in Figure 3. The corresponding area profiles obtained using the method described in section 4 are also plotted, and the values of a_4 and a_5, a_6 used are given in Table 2.

TABLE 2

Constants used in generating mode shapes for Figure 3

	1	2	3	4	5
a_4	1000	1000	1000	1000	1000
a_5	100	− 373	− 845	− 1318	− 1791
a_6	0	1	2	3	4

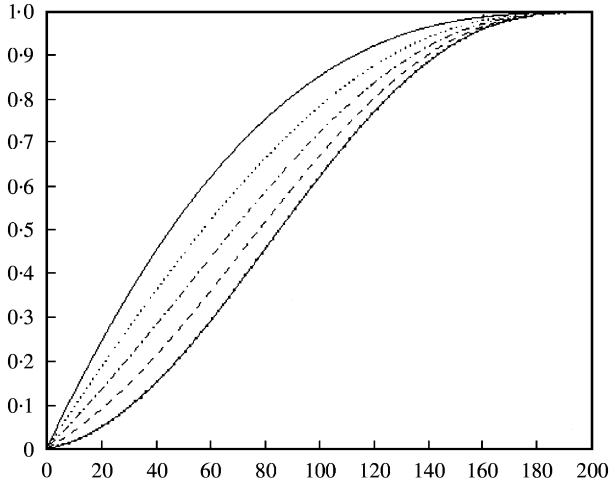

Figure 4. The first derivative of the mode shapes shown in Figure 3: ——, $a_6 = 0$; . . . ., 1; —·—, 2; – – –, 3; ——, 4.

Figure 4 shows that the first derivative of the selected mode shapes that satisfy criterion (3) where the number of sign changes of the mode shape and the first derivatives are both zero.

7. STRUCTURAL DESIGN METHOD FOR DESIRED MODE SHAPES

Since not all arbitrarily specified mode shapes yield physically realizable geometries, when a specified mode shape does not satisfy the criteria for physical realizability, it should be modified with minimal alteration using an optimization method. Such a method is presented below for cantilever beams. In order to find the closest match to a specified mode shape that will satisfy the four criteria for physical realizability of beam geometries, a least squares formulation is used here. A function of an assumed form, with some adjustable parameters such as a polynomial whose coefficients can be adjusted, is used to match the specified mode shape. The objective function used here is a measure of *goodness* of match between the specified mode shape and the modified mode shape. The optimization variables are the adjustable parameters in the mode shape function of an assumed form. Starting from an initial guess, the optimization variables are updated to minimize the deviation between the prescribed and modified mode shapes as

$$\min_{a_4, a_5, a_6} \sum_{i=1}^{N} (u_{specified} - u_{modified})_i^2, \tag{28}$$

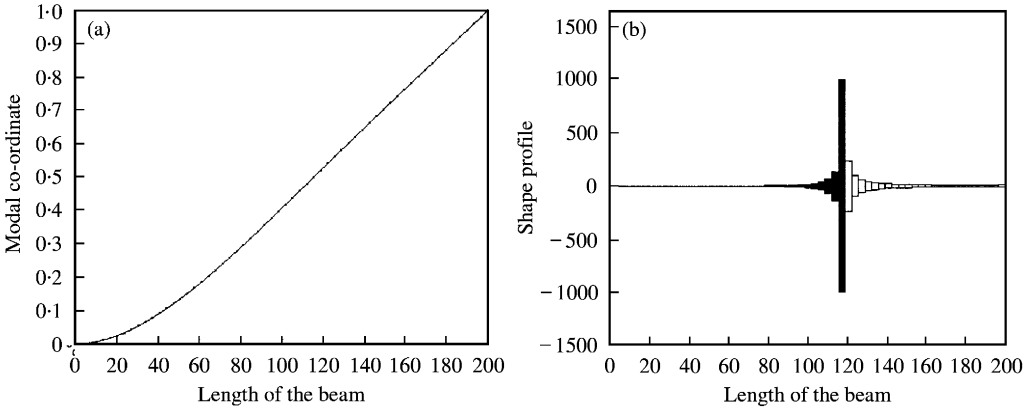

Figure 5. (a) An arbitrarily specified prescribed sixth degree polynomial mode shape. (b) Shape profile generated from the prescribed mode shape. White elements are negative shape profile elements, which are physically unrealizable. Black elements denotes show positive portions.

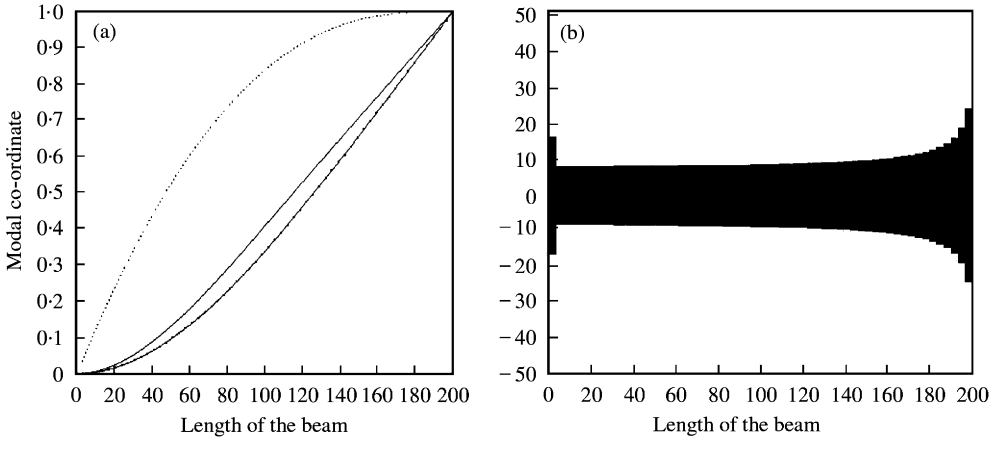

Figure 6. (a) Original and modified mode shapes and the first derivative of the modified mode shape; (b) shape profile generated from the modified mode shape; ——, prescribed mode shape; •—•, polynomial-based mode shape; . . . . ., first derivative of the polynomial mode shape.

where $u_{specified}$ is the prescribed mode shape, $u_{modified}$ is the polynomial-based mode shape and N is the number of points used to compute the deviation. An example is presented below to illustrate how a user-supplied mode shape that does not satisfy the four criteria is modified via the optimization method to yield the closest physically realizable shape. A prescribed mode shape was given as a polynomial below and is shown in Figure 5:

$$u(x) = 1{\cdot}0265e10x^2 - 94\,320\,000x^3 + 100x^4 - 2636x^5 + 10x^6. \tag{29}$$

When the method described in section 4 was used, the shape profile shown in Figure 5 is obtained with some negative values. Upon evaluating the prescribed mode shape against the four criteria, the mode shape is altered so that that is the closest match to the prescribed shape is obtained. The resulting polynomial-based mode shape has parameters, $a_4 = 100{\cdot}59$, $a_5 = -2248{\cdot}8$, and $a_6 = 1{\cdot}7010e5$ and is shown in Figure 6(a). The first

derivative of the polynomial-based mode shape is also plotted in the figure. The shape profile obtained using this modified mode shape is shown in Figure 6(b).

8. CONCLUSION

The *design* problem of determining the geometry of a structure for desired mode shape is the focus of this paper. Methods of reconstructing the shape profile of both bars and beams for a desired mode shape were discussed. Because not all desired mode shapes yield physically realizable shape profile, a set of criteria for the mode shapes that ensure physical realizability are identified for bars and cantilever beams. For the desired mode shapes that do not satisfy the criteria, an optimization-based method was used to find the closest matching physically realizable mode shape. Future work will address other cases of beams and other regular members such as curved beams, plates and shells.

REFERENCES

1. M. Chu 1992 *SIAM Review* **40**, 1–39. Inverse eigenvalue problems.
2. Z.-D. Ma, N. Kikuchi, H.-C. Cheng and I. Hagiwara 1995 *American Society of Mechanical Engineers Journal of Applied Mechanics* **62**, 200–207. Topological optimization technique for free vibration problems.
3. M. W. Putty and K. Najafi 1994 *Technical Digest*, *Sensors and Actuators Workshop*, *Hilton Head Islands*, *SC*, *June* 13–16, 213–220. A micromachined vibrating ring gyroscope.
4. N. Pedersen 2000 *Engineering Optimization* **32**, 373–392. Design of cantilever probes for atomic force microscopy (AFM).
5. J. P. Ostrowski 1996. Private communication, University of Pennsylvania.
6. R. G. Ross 1971 *SAE Paper 710787* 2627–2635. Synthesis of stiffness and mass matrices from experimental vibration modes.
7. G. M. L. Gladwell 1984 *Proceedings of the Royal Society of London A* **393**, 277–295. The inverse problem for the vibrating beam.
8. G. M. L. Gladwell 1986 *Inverse Problem in Vibration*. Dordrecht: Martinus Nijhoff.
9. G. M. L. Gladwell 1986 *Proceedings of the Royal Society of London A* **407**, 199–218. The inverse problem for the Euler–Bernoulli beam.
10. Y. M. Ram and J. Calwell 1992 *SIAM Journal of Applied Mathematics* **52**, 140–152. Physical parameters reconstruction of a free–free mass spring system from its spectra.
11. Y. M. Ram 1993 *SIAM Journal of Applied Mathematics* **53**, 1762–1775. Inverse eigenvalue problem for a modified vibrating system.
12. Y. M. Ram 1994 *American Society of Mechanical Engineers Transactions Journal of Applied Mechanics* **61**, 624–628. An inverse mode problem for the continuous model of an axially vibrating rod.
13. Y. M. Ram 1994 *Journal of Sound and Vibration* **169**, 239–252. Inverse mode problems for the discrete model of a vibrating beam.
14. Y. M. Ram and G. M. L. Gladwell 1994 *Journal of Sound and Vibration* **169**, 229–237. Constructing a finite element model of a vibratory rod from eigendata.
15. E. K. Lai and G. K. Ananthasuresh 1998 *American Society of Mechanical Engineers Design Engineering Technical Conferences*, *Atlanta*, *Georgia*, *September* 13–16, *DETC*98/*DAC*-5632. Design for desired mode shapes—preliminary results.
16. N. Levinson 1945 *Matematicheskii Tidsskrift B* 25–30. The inverse Sturm–Liouville problem.
17. O. H. Hald 1978 *Mathematics of Computation* **32**, 687–705. The inverse Sturm–Liouville problem and the Rayleigh Ritz method.
18. B. M. Levitan 1968 *American Mathematical Society—Translations* **68**, 1–20. On the determination of a Sturm–Liouville equation by two spectra.
19. H. Hochstadt 1974 *Linear Algebra and Applications* **8**, 435–446. On the construction of a Jacobi matrix from spectral data.
20. V. Barcilon 1979 *SIAM Journal of Applied Mathematics* **37**, 605–613. On the multiplicity of solutions of the inverse problem for a vibrating beam.

21. V. BARCILON 1979 *Journal of Applied Mathematics and Physics* **24**, 346–358. On the multiplicity of solutions of the inverse problem for a vibrating beam.
22. V. BARCILON 1982 *Philosophical Transactions of the Royal Society of London A* **304**, 211–252. Inverse problems for the vibrating beam in the free-clamped configuration.
23. G. M. L. GLADWELL 1985 *Journal of Mechanics and Applied Mathematics* **39**, 297–307. The inverse mode problems for lumped-mass systems.
24. G. M. L. GLADWELL and J. A. GBADEYAN 1985 *Quarterly Journal of Mechanics and Applied Mathematics* **38**, 169–174. On the inverse problem of the vibrating string and rod.